

CO2Capture through Aqueous Carbonation Using Green Liquor Dregs as the Absorbent

Downloaded from: https://research.chalmers.se, 2025-11-29 09:43 UTC

Citation for the original published paper (version of record):

Couto Queiroz, E., Leventaki, E., Kugge, C. et al (2025). CO2Capture through Aqueous Carbonation Using Green Liquor Dregs as the Absorbent. ACS Sustainable Resource Management, 2(1): 119-126. http://dx.doi.org/10.1021/acssusresmgt.4c00373

N.B. When citing this work, cite the original published paper.

research.chalmers.se offers the possibility of retrieving research publications produced at Chalmers University of Technology. It covers all kind of research output: articles, dissertations, conference papers, reports etc. since 2004. research.chalmers.se is administrated and maintained by Chalmers Library

Süstainable

Resource Management

CO₂ Capture through Aqueous Carbonation Using Green Liquor Dregs as the Absorbent

Eduarda C. Queiroz,* Emmanouela Leventaki, Christian Kugge, and Diana Bernin



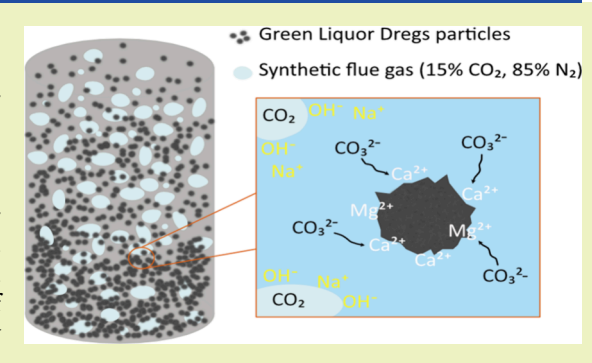
Cite This: ACS Sustainable Resour. Manage. 2025, 2, 119–126



ACCESS

III Metrics & More

ABSTRACT: Industrial side streams can be used to capture CO₂ due to the presence of metals such as Ca, Mg, Na, and others. Green liquor dregs (GLD), an industrial alkaline solid waste generated by pulp and paper companies, can capture CO₂ through aqueous direct carbonation. However, aqueous carbonation requires high water consumption. To address this, an alkaline wastewater from the pulp and paper industry was used as an alternative to fresh water, reducing the need for additional water consumption. In this work, the absorption capacities, reaction yield, and physicochemical characteristics of the samples were studied. A 3D-printed reactor, designed by our research group, was used to take advantage of bubble turbulence for mixing the aqueous and gaseous phases, thereby reducing electricity consumption. The solids before and after carbonation



Article Recommendations

were analyzed using X-ray diffraction and scanning electron microscopy. The absorption capacity for GLD in deionized water was in the range between 5.92 and 14.86 g/L, while for GLD in wastewater, it was between 8.11 and 17.81 g/L. These results indicate that the presence of wastewater can enhance CO_2 absorption. Physicochemical analysis confirmed the presence of $CaCO_3$ after the reaction.

KEYWORDS: carbon capture, absorption capacity, alkaline wastewater, waste utilization, CO₂ reduction, green liquor dregs

INTRODUCTION

Global warming and its effects are becoming more prominent every year¹ and sustainable technologies are evolving at a very slow rate, the need to provide drastic, innovative solutions is growing. To reach the target of zero greenhouse gas emissions, a series of synergistic technologies will need to be implemented.²

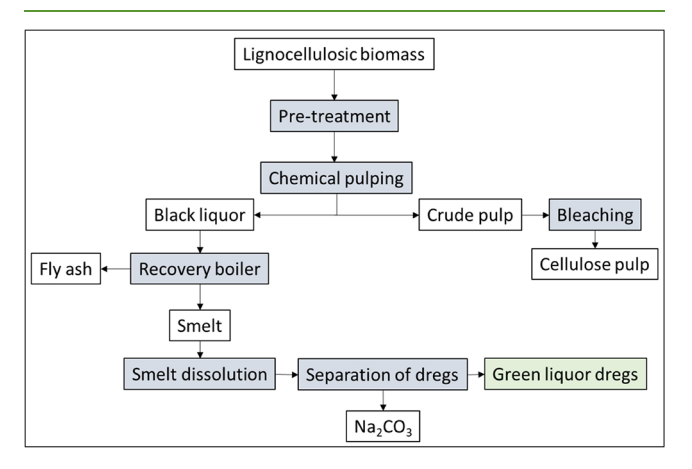


Figure 1. Simplified scheme of a typical industrial paper and pulp process from the raw material until the separation of GLD, modified from refs 14 and 15.

Renewable energy sources are the key to a smooth transition from the current fossil-based energy systems, but other technologies, such as carbon capture, will also be an essential addition to inhibit the emission of more CO_2 during the transition. The principle of carbon capture is to prevent industrially generated CO_2 from getting released in the environment. In theory, this could be a useful temporary measure to keep the atmospheric levels of CO_2 stable during the energy transition. Unfortunately, implementation is still limited because carbon capture technologies are quite costly from a techno-economic perspective.³

One approach that could potentially abate this problem is the use of alkaline waste materials to capture this gas. The capture of CO_2 using alkaline waste has gained a lot of attention over the years, as it targets both the mitigation of CO_2 emissions and the valorization of industrial side streams. These streams owe their alkalinity to a high content of metal oxides, such as CaO_1 , MgO_2 , and others. Metal oxides can readily react with CO_2 toward the

Received: September 16, 2024
Revised: December 5, 2024
Accepted: December 5, 2024
Published: December 17, 2024





formation of metal carbonates, in a process called carbonation or mineralization. 5 Carbonation occurs naturally between the CO_2 in atmospheric air and alkali minerals, but this reaction is extremely slow. 6 To accelerate this process water can be used as a medium to dissolve the metal oxides and facilitate the interaction between dissolved compounds coming from the industrial side streams and CO_2 . This technology has been proposed as a solution to the decarbonization of post-combustion flue gases. 7 Industrial side streams that have been explored for this purpose include steelmaking slags, municipal solid waste incinerator ashes, cement kiln dust, and more. $^{4,8-11}$

Side streams coming from heavy industries, such as steelmaking slag, have been studied extensively as their use for carbon capture offers an opportunity to build up the industries' sustainability and decrease their carbon footprint. 12,13 However, there are plenty of other side streams that have not gained much attention, but could nevertheless prove to be attractive candidates for carbon capture. An example of this is green liquor dregs (GLD), a residue of the paper and pulp industry.¹⁴ GLD derive from the cooking process that delignifies wood to separate cellulosic pulp, as displayed in Figure 1. The byproduct of the cooking process is black liquor, an aqueous mixture of organic biomolecules and cooking chemicals. Black liquor is then transferred to the recovery boiler which generates green liquor and GLD. The green liquor is further treated to recover pure cooking liquor which is recycled back into the process, but the GLD are disposed in landfill.¹⁴

GLD typically contain CaO, MgO, Na₂O, and K_2O as well as SiO₂, Al₂O₃, Fe₂O₃, and other compounds in smaller concentrations. ¹⁶ This composition makes them interesting candidates for carbon capture via carbonation, but to our knowledge, this possibility has not been pursued. Only very limited research exists on the utilization of this material to seal mine waste deposits. ^{17,18}

 $\rm CO_2$ capture can occur by direct carbonation and indirect carbonation. Direct carbonation can be divided into aqueous and gas—solid carbonation. In this work, direct aqueous carbonation was used because it offers advantages such as faster dissolution of $\rm Ca^{2+}$ and $\rm Mg^{2+}$, resulting in increased reaction rate, reduced process costs, minimized chemical usage, and the avoidance of high temperatures and pressures. ¹⁹ The chemical reaction between the metal oxides with $\rm CO_2$ in aqueous solution occurs in various steps. The equations are provided as follows: 10,20,21

(1) CO₂ dissolves in water and forms carbonic acid:

$$CO_2(g) + H_2O(l) \rightleftharpoons H_2CO_3(aq)$$
 (1)

(2) Carbonate and bicarbonate ions are forming in the solution:

$$H_2CO_3(aq) \rightleftharpoons HCO_3^-(aq) + H^+(aq)$$
 (2)

$$HCO_3^-(aq) + OH^-(aq) \rightleftharpoons H_2O(l) + CO_3^{2-}(aq)$$
(3)

(3) Metal ions dissolve in the solution:

$$CaSiO_3(s) + 2H^+(aq)$$

 $\rightarrow Ca^{2+}(aq) + SiO_2(s) + H_2O(l)$ (4)

$$CaO(s) + H_2O(1)$$

 $\Rightarrow Ca(OH)_2(s)$
 $\Rightarrow Ca^{2+}(aq) + 2OH^{-}(aq)$ (5)

$$MgO(s) + H_2O(l)$$

 $\rightleftharpoons Mg(OH)_2(s)$
 $\rightleftharpoons Mg^{2+}(aq) + 2OH^{-}(aq)$ (6)

(4) Formation of metal carbonates:

$$Ca^{2+}(aq) + CO_3^{2-}(aq) \to CaCO_3(s)$$
 (7)

$$Mg^{2+}(aq) + CO_3^{2-}(aq) \rightarrow MgCO_3(s)$$
 (8)

In this study, the absorption of CO_2 from synthetic flue gas in GLD was investigated. Experiments were conducted using both deionized water and alkaline wastewater from the same industry as the aqueous medium. The aim was to study whether fresh water could be replaced by a wastewater available at the same industrial site and assess if the presence of other elements could influence CO_2 absorption. Direct aqueous carbonation was used to promote the leaching of metal ions in the solution and accelerate the carbonation process at ambient temperature and pressure. The experiments took place in a semibatch bubble column reactor, where the gaseous phase, consisting of 15% CO_2 and 85% N_2 was constantly flowing, and the liquid phase contained the mixture of GLD in water.

EXPERIMENTAL SECTION

Materials. Samples of GLD and alkaline wastewater were provided by SCA in Sundsvall, Sweden. The composition of GLD is given in Table 1.

Table 1. Main Composition of the GLD

| chemical | composition (TS %) ^a |
|---|---------------------------------|
| CaO | 25 |
| MgO | 12.5 |
| SiO_2 | 1.86 |
| Al_2O_3 | 0.918 |
| Fe_2O_3 | 0.435 |
| MnO | 2.44 |
| Na ₂ O | 3.76 |
| annual production in Sweden (t) ¹⁸ | ~240000 |
| The material has 45% total solids (TS) | |

^aThe material has 45% total solids (TS).

The average particle size of GLD is 0.09 cm. To evaluate the $\rm CO_2$ absorption of the material in its as-received condition, it was left uncrushed. Particle size measurements were obtained from SEM images and pictures of the particle and analyzed with Fiji (ImageI) software.

The wastewater comes from a combination of water streams generated through the pulping process, and it mainly contains NaOH, Na₂S, Na₂S₂O₃, Na₂SO₄, Na₂CO₃, and KSO₃.

Methods. The GLD samples were mixed with 60 mL of water at solid/liquid (S/L) ratios of 50, 100, 150, and 200 g/L. The mixture was stirred for 24 h for all concentrations at 400 rpm. After stirring, the mixture was transferred to the reactor. This reactor was customized by Leventaki et al. to utilize the motion of the gas bubbles to generate turbulence and induce mixing between the gaseous and aqueous phases. The reactor was 3D-printed using a stereolithography 3D printer (Form 3+, Formlabs) and designed with Autodesk Fusion 360.

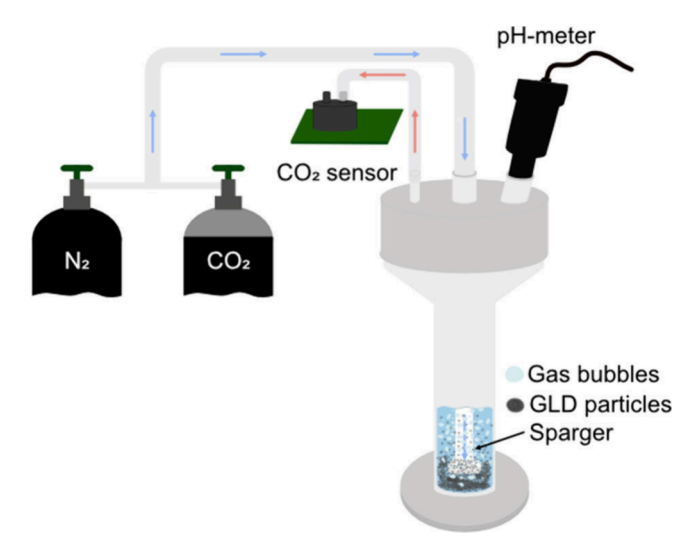


Figure 2. Schematic diagram of the experimental setup.

The gas flow rate was maintained at 200 mL/min, with a gas composition of 15% CO $_2$ and 85% N_2 . This concentration was controlled using two Mass Flow Controllers (MFC) from Brooks Instrument, the flow rate and composition of the final mixture were adjusted using a standalone controller (0254, Brooks Instrument). To determine the absorption of CO $_2$, a CO $_2$ sensor (ExplorIR, GSS) was employed, measuring the concentration of CO $_2$ at the outlet of the reactor every 5 s. The reaction was considered finished when the CO $_2$ sensor reached $\sim\!15\%$ CO $_2$. A pH probe (HQ430D, HACH) was inserted in the mixture and measured the pH every 10 s. Figure 2 shows the setup of the experiment. The reaction was performed at room temperature and 1 atm pressure. After the experiment, the precipitated solids were dried in an oven for 3 days at 50 °C. Furthermore, some carbonation experiments were repeated with the pH meter and an FTIR probe (ReactIR 702L, Mettler Toledo) immersed in the mixture to monitor the formation of CO $_3^{2-}$ and HCO $_3$ by measuring every 10 s. Measurements using XRD and SEM were conducted for the

Measurements using XRD and SEM were conducted for the concentration of 50 g/L. The powder was analyzed using a Bruker XRD model D8 Discover instrument, over a diffraction angle range from 10 to 70° with a scan step of 0.02°/s. SEM images were recorded at 20 kV using a FEI Quanta 200 FEG ESEM instrument, and to increase the conductivity of the images, a layer of gold with a thickness of 4 nm was deposited onto the samples.

RESULTS AND DISCUSSION

CO₂ Absorption for Deionized Water and Wastewater.

Initially, experiments were conducted with sparging gas through pure deionized water and the wastewater to evaluate the absorption of CO₂ in each medium without the addition of GLD. Figure 3 shows the CO₂ absorption and pH over time for both deionized water and wastewater. The pH of the deionized water is 6.67. During the experiment the pH decreases to 5.48 within the first minute due to the formation of H_2CO_3 (reaction 1) and subsequent ionization of this acid, forming H⁺ and HCO₃⁻ (reactions 2 and 3). The CO₂ solubility in deionized water is 0.89 g/L at 22 °C. In contrast, wastewater presents an initial pH value of 10.44, attributed to the presence of alkaline compounds, such as NaOH. The pH drops to 10 as the CO₂ reacts with OH⁻, which is in excess, leading to the formation of CO₃²⁻. Following that, formation of HCO₃⁻ occurs mainly within the pH range of 7-10 because CO₃²⁻ that is already in the solution follows the opposite direction of reaction 3, generating more $HCO_3^{-20,21}$ The equivalence point of the reaction occurs at pH 8.3, where the reactants are in

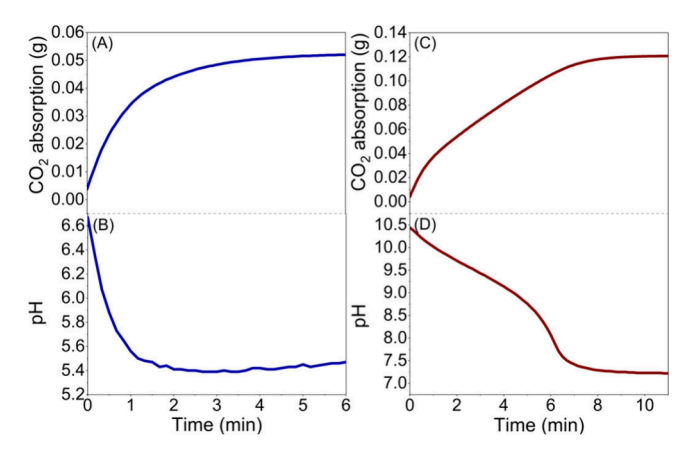


Figure 3. (A) CO₂ absorption and (B) pH over time for 60 mL of deionized water and (C) CO₂ absorption and (D) pH over time for 60 mL of wastewater.

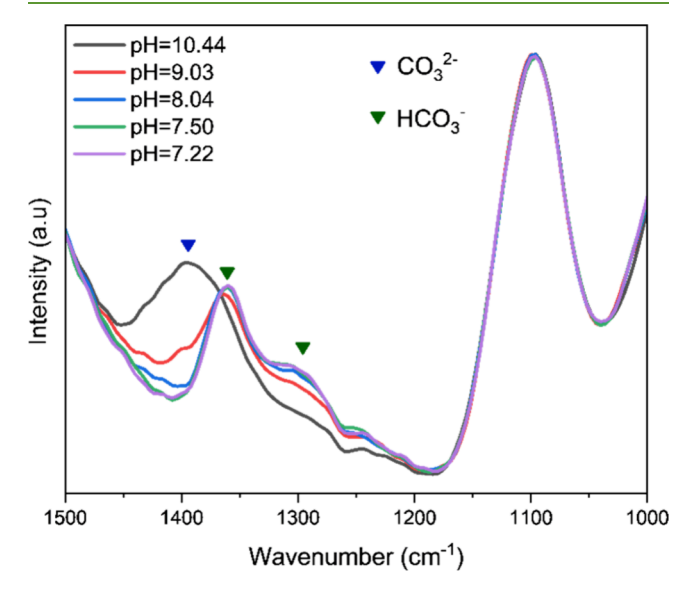


Figure 4. FTIR spectra of wastewater monitored at varying pH levels during a carbonation experiment.

stoichiometric balance according to the chemical equation. The end point of the reaction is reached at pH 7.22.

The CO_2 absorption of wastewater is 2.04 g/L. However, the solubility of CO_2 in water is 0.89 g/L, so the capture chemical absorption of CO_2 in the wastewater, due to the presence of alkaline compounds is actually 1.15 g/L.

Figure 4 presents the FTIR spectra of wastewater monitored throughout the experiment. The initial wastewater spectrum at pH 10.44 shows a prominent band at 1396 cm⁻¹, corresponding to $\rm CO_3^{2-}$. As the pH decreases, a new absorption band appears at 1360 cm⁻¹, with a shoulder at 1300 cm⁻¹, indicating the formation of $\rm HCO_3^{-}$ and, consequently, the $\rm CO_3^{2-}$ band at 1396 cm⁻¹ diminishes as the concentration of this ion decreases. At the end of the reaction, the band of $\rm HCO_3^{-}$ exhibits maximum intensity.

CO₂ Absorption for GLD. Figure 5 shows the CO₂ absorption and evolution of the pH for GLD in deionized water and wastewater. It can be observed that higher concentration of solids leads to enhanced absorption of CO₂ and longer reaction time. This occurs for the GLD in deionized water and wastewater. The CO₂ absorption and yield for GLD are shown in Table 2.

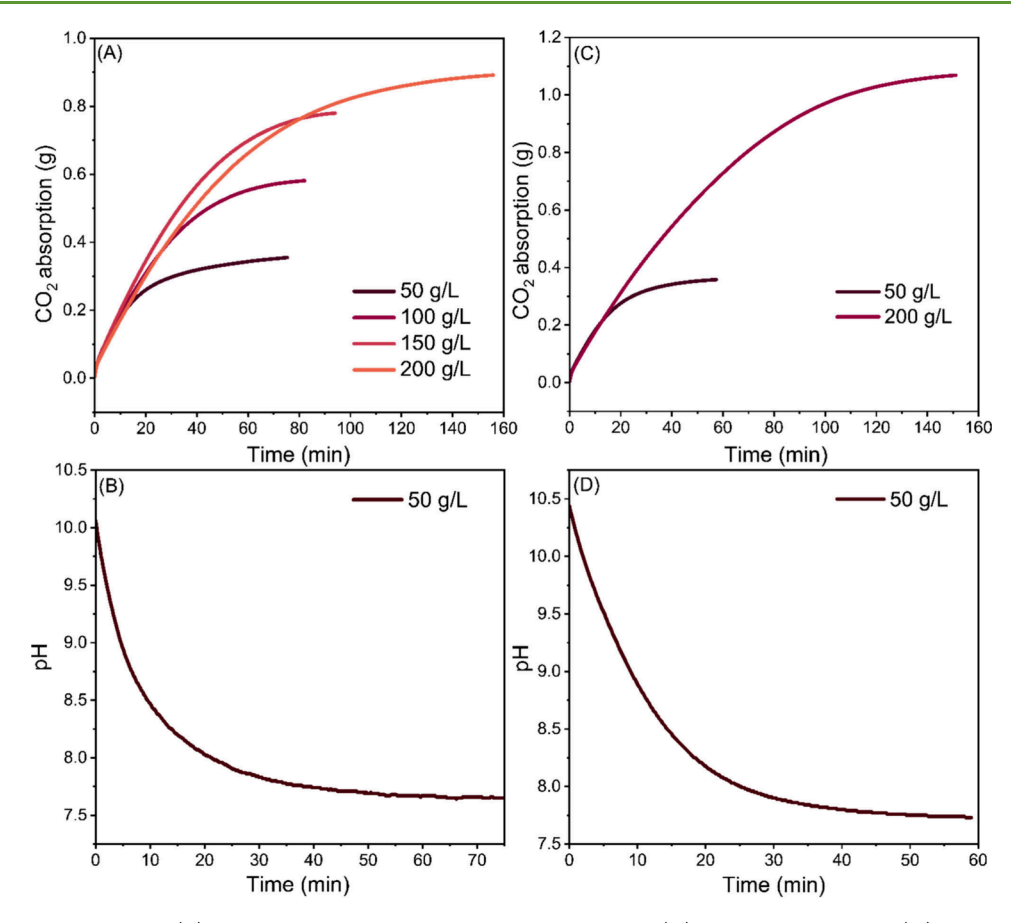


Figure 5. (A) CO₂ absorption and (B) pH over time for GLD in deionized water and (C) CO₂ absorption and (D) pH over time for GLD in wastewater.

Table 2. Absorption and Yield for GLD with Deionized Water and GLD with Wastewater after Carbonation

| absorbent system | absorption (g/L) | yield (g/g) |
|------------------------------|------------------|---------------|
| GLD in deionized water (g/L) | | |
| 50 | 5.92 | 0.114 |
| 100 | 9.69 | 0.097 |
| 150 | 13.00 | 0.087 |
| 200 | 14.86 | 0.074 |
| GLD in wastewater (g/L) | | |
| 50 | 8.11 | 0.162 |
| 200 | 17.81 | 0.089 |

An increase in the S/L ratio leads to a reduction in the dissolution of ${\rm Ca}^{2+}$, ${\rm Mg}^{2+}$, and ${\rm CO}_2$, due to the reduced moisture content on the reaching of maximum solubility of the compounds. This relationship is supported by the data presented in Table 2, indicating that higher S/L ratios correspond to lower carbonation yields for the materials.

For the GLD in wastewater, it appears that the presence of Na^+ improves the CO_2 absorption, as can be observed when comparing both the absorption and yield for 50 and 200 g/L between the deionized water and wastewater mixtures. In mixtures containing wastewater, the pH drops more slowly compared to mixtures with deionized water. In the mixture with wastewater, the pH remains higher than 8 for 25 min, while in the mixture with deionized water, the pH remains above 8 for 8.33 min. Furthermore, the initial pH of GLD in wastewater is higher than the pH of GLD in deionized water, which can

contribute to the increase in ${\rm CO_2}$ absorption, as the carbonation yield is pH-dependent.

For both 50 and 200 g/L concentrations, GLD mixtures in deionized water present a lower yield compared to GLD in wastewater. The presence of Na₂CO₃ in the wastewater can explain these differences, as Na₂CO₃ creates an indirect route for the carbonation reaction of CaO·SiO₂ (eq 9):²⁴

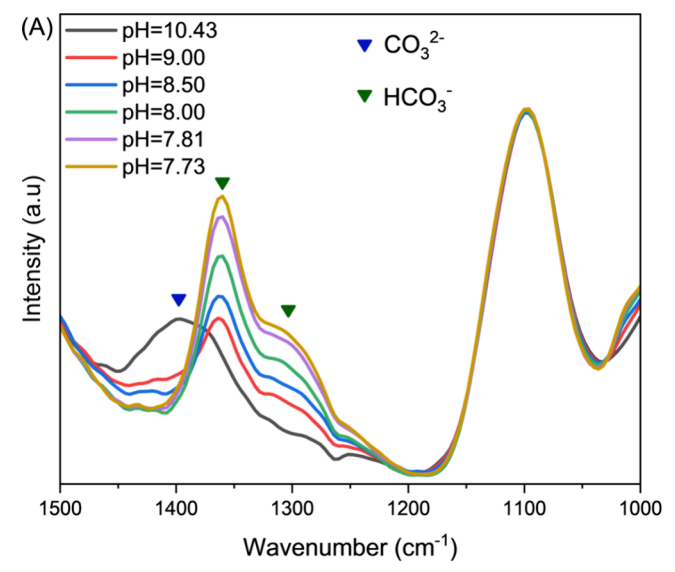
$$2\text{CaO} \cdot \text{SiO}_2(s) + 2\text{Na}_2\text{CO}_3(\text{aq}) + 2\text{H}_2\text{O}(l)$$

 $\rightarrow 2\text{CaCO}_3(s) + \text{SiO}_2(s) + 4\text{NaOH}(\text{aq})$ (9)

This reaction increases the formation of $CaCO_3$ from $Ca\cdot SiO_2$. Furthermore, the formation of OH^- creates an autocatalytic basification process, raising the pH and enhancing CO_2 absorption.²⁵

The formation of HCO_3^- and CO_3^{2-} can be analyzed using FTIR spectroscopy. Figure 6 shows the FTIR spectra of GLD in wastewater and deionized water. The spectra reveal the presence of CO_3^{2-} in the GLD wastewater mixture, as indicated by the characteristic band at 1396 cm⁻¹, which is absent in the GLD deionized water sample. When the pH reaches 9, a band at 1360 cm⁻¹ and a shoulder at 1304 cm⁻¹ appear in both mixtures, while the CO_3^{2-} band decreases in intensity. The intensity of this band increases throughout the reaction, reaching a maximum at pH 7.73 for GLD in wastewater and pH 7.64 for GLD in deionized water. These results indicate that it is possible to absorb more CO_2 using the alkaline wastewater from the industry with less material.

XRD and SEM Analysis. Figure 7 shows the XRD patterns before and after the carbonation experiments for wastewater,



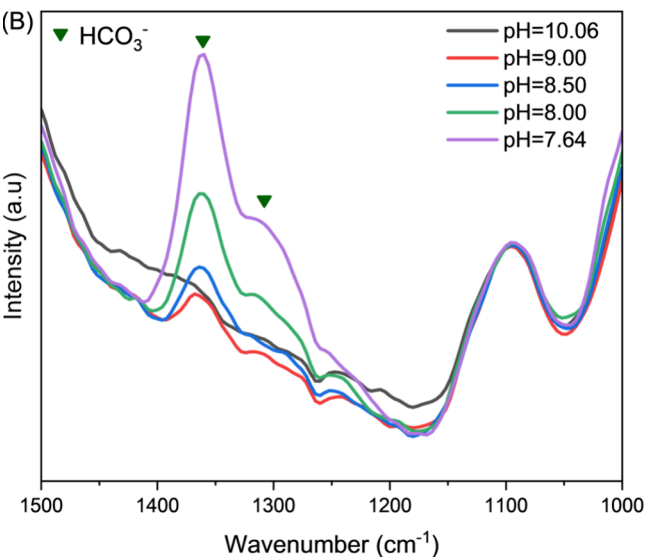


Figure 6. FTIR spectra of GLD in (A) wastewater and (B) deionized water, monitored at varying pH levels during a carbonation experiment.

GLD in deionized water, and GLD in wastewater. The wastewater contains NaOH, Na₂S, Na₂S₂O₃, Na₂SO₄, KSO₃, and Na₂CO₃ from the Kraft pulping process. After carbonation, the intensity of the peaks corresponding to NaOH and Na₂CO₃ decreases, while NaHCO₃ peaks appear, indicating the consumption of NaOH and Na₂CO₃ and the formation of NaHCO₃. GLD in deionized water presents peaks corresponding to CaCO₃ and MnO(OH). After carbonation, the peak for MnO(OH) persists in XRD for all concentrations, suggesting that MnO(OH) does not participate in the carbonation reaction. CaCO₃ peaks remain evident in the XRD, consistent with the crystalline phase structure of calcite. Additionally, a peak at 32 (2 θ degrees) indicates the presence of MgCO₃·3H₂O. These peaks signify the formation of MgCO₃·3H₂O and the presence of CaCO₃.

GLD in wastewater shows peaks for CaCO $_3$ and MnO(OH) from GLD before carbonation, as well as peaks for Na $_2$ S, Na $_2$ SO $_4$, and KSO $_3$ from the wastewater. After carbonation, peaks for NaHCO $_3$ and MgCO $_3$ ·3H $_2$ O appear. The peaks for CaCO $_3$ and MgCO $_3$ ·3H $_2$ O correspond to calcite and nesquehonite, respectively.

The morphology of the samples was analyzed using SEM. Figure 8A presents the SEM image of the dried wastewater before carbonation. The EDS shows that the solid contains Na, S, O, and K. After carbonation (Figure 8B), a spherical morphology formed from needles of NaHCO₃ can be observed, which can be confirmed by the percentages of Na, O, and C obtained in the EDS analysis.²⁹

GLD in deionized water before carbonation demonstrates the flower-like morphology of Mg(OH)2 and rhombohedral morphology from CaCO₃ in Figure 9A. After the carbonation, the image shows rhombohedral morphology from CaCO3 that corresponds to calcite in Figure 9B. For high concentrations of GLD (200 g/L), crystalline structures were formed in the surface of the solids (Figure 9C). The SEM of these crystals presents a needlelike morphology from MgCO₃·3H₂O, which corresponds to nesquehonite. MgCO₃·3H₂O grows on the petals of Mg(OH)₂ and forms a bundle-like MgCO₃·3H₂O (Figure 9D). 30 GLD in wastewater before carbonation (Figure 10A) exhibits a square morphology characteristic of CaCO₃ from GLD. After carbonation (Figure 10B), deposits of Na₂CO₃ and NaHCO₃ are observed, with their compositions confirmed by EDS, resulting from the formation of a layer on top of the calcite due to the deposition of these materials during the drying process. This deposition hinders the visualization of the calcite. To improve calcite visualization, the mixture after carbonation was filtered, and the solid was dried separately, excluding the solution containing Na₂CO₃ and NaHCO₃. Consequently, the square morphology of calcite from GLD in wastewater after carbonation became visible (Figure 11). This occurs because Na₂CO₃ and NaHCO₃ are water-soluble, and during the drying process in the oven, they deposit on top of CaCO₃.

CONCLUSIONS

In this study, the physicochemical characteristics, absorption capacities, and yields were determined for GLD in various concentrations in both deionized water and wastewater. The experiments were conducted using a 3D-printed reactor, which eliminates the energy expenses associated with stirring. GLD in deionized water at 50 and 200 g/L exhibited CO2 absorption of 5.92 and 14.86 g/L, respectively. In wastewater, GLD at 50 and 200 g/L showed CO₂ absorption of 8.11 and 17.81 g/L, respectively. These values indicate that using wastewater instead of deionized water can reduce freshwater consumption and enhance GLD absorption in wastewater. Furthermore, because GLD is landfill material, the predominant carbonation product was found to be CaCO₃, indicating potential applications for the carbonated products as binders in cementitious materials or as fillers for paper and linerboard, potentially with optimized mineral morphology and abrasiveness. These findings suggest that GLD and wastewater can be effectively utilized for aqueous carbonation, thereby reducing water wastage by incorporating wastewater from industrial processes.

AUTHOR INFORMATION

Corresponding Author

Eduarda C. Queiroz — Department of Chemistry and Chemical Engineering, Chalmers University of Technology, SE-41296 Gothenburg, Sweden; orcid.org/0000-0002-5239-3518; Email: eduarda@chalmers.se

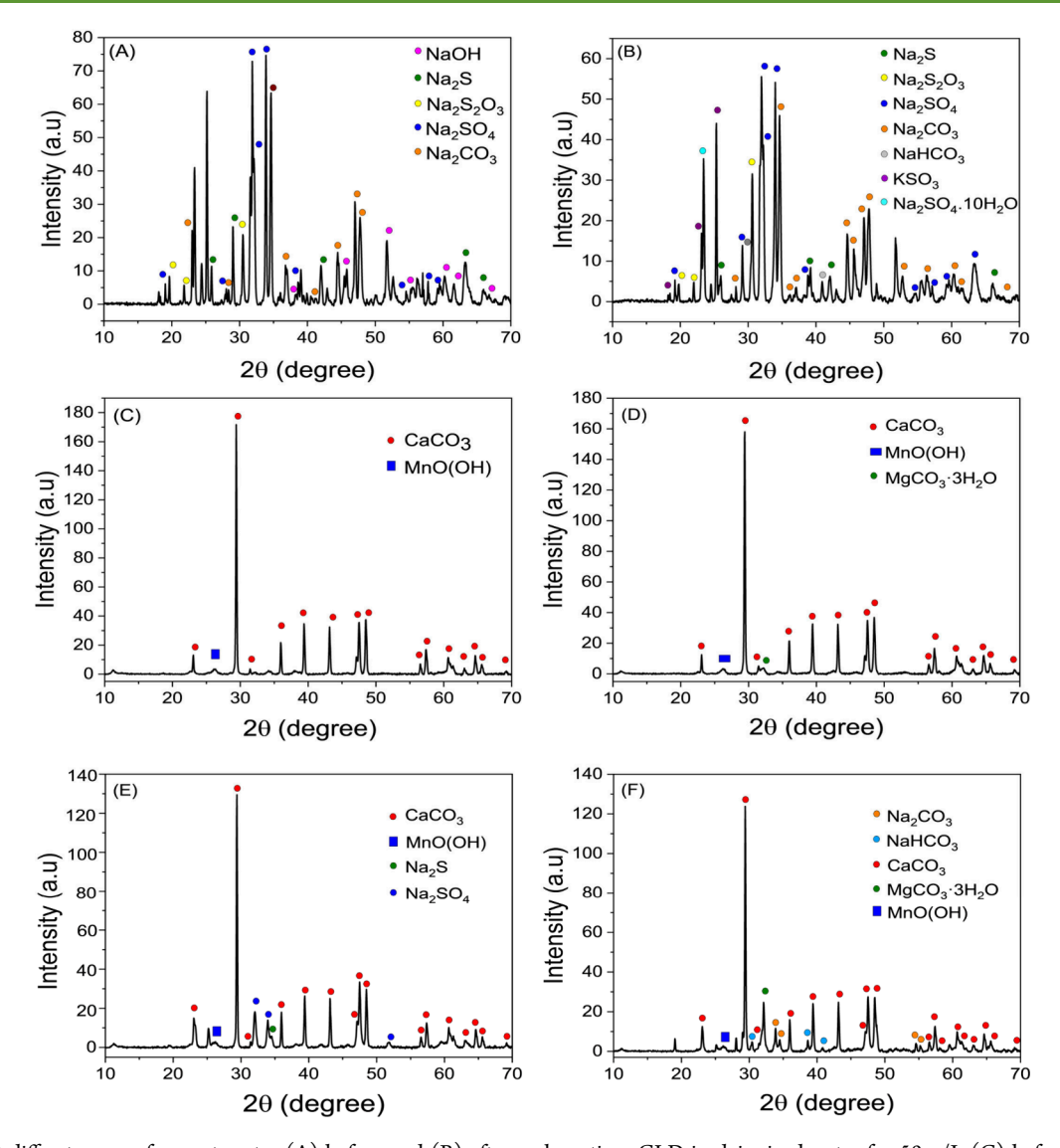


Figure 7. XRD diffractograms for wastewater (A) before and (B) after carbonation, GLD in deionized water for 50 g/L (C) before and (D) after carbonation, and GLD in wastewater for 50 g/L (E) before and (F) after carbonation.

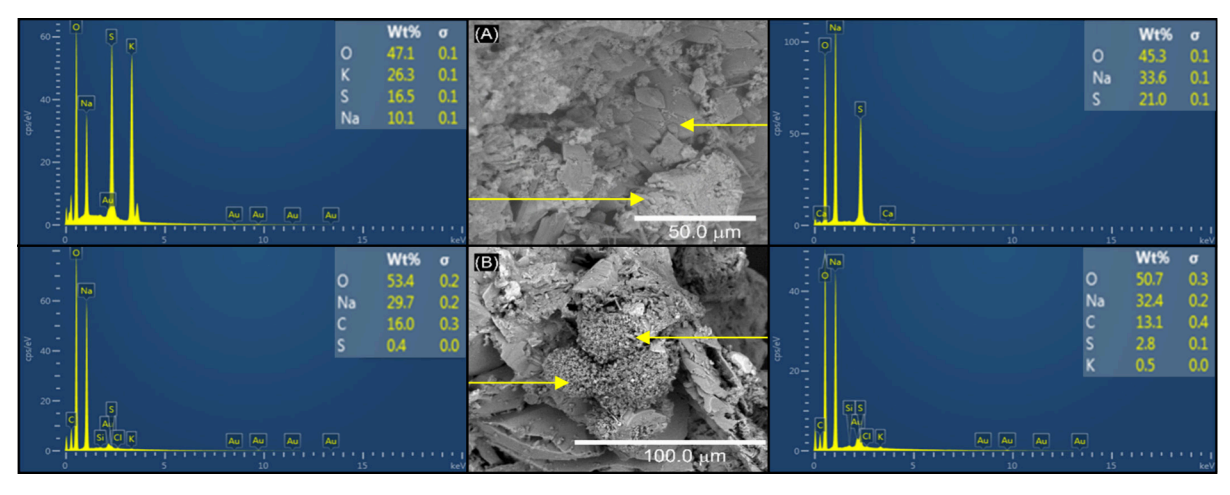


Figure 8. SEM images for the powders from wastewater (A) before and (B) after carbonation.

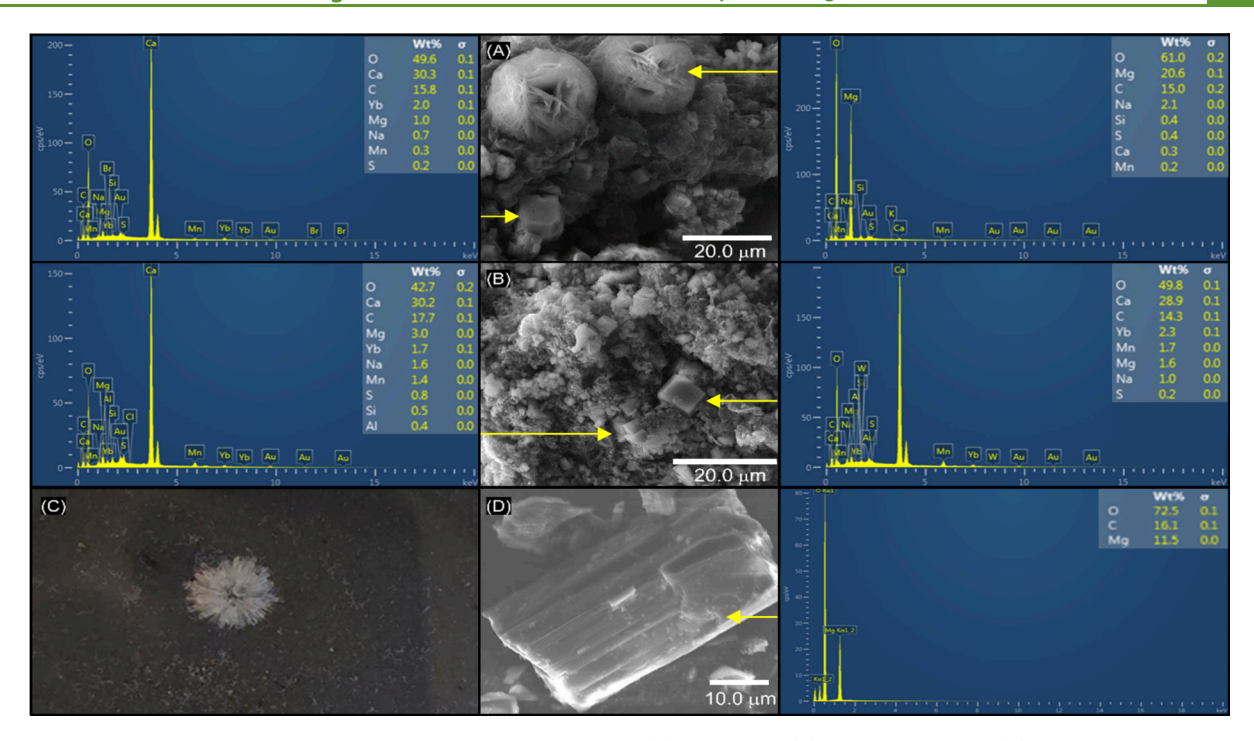


Figure 9. SEM images for the powders GLD in deionized water at 50 g/L (A) before and (B) after carbonation. (C) Picture of the $MgCO_3$ · $3H_2O$ crystal obtained from the reaction at a concentration of 200 g/L. (D) SEM images of the crystal.

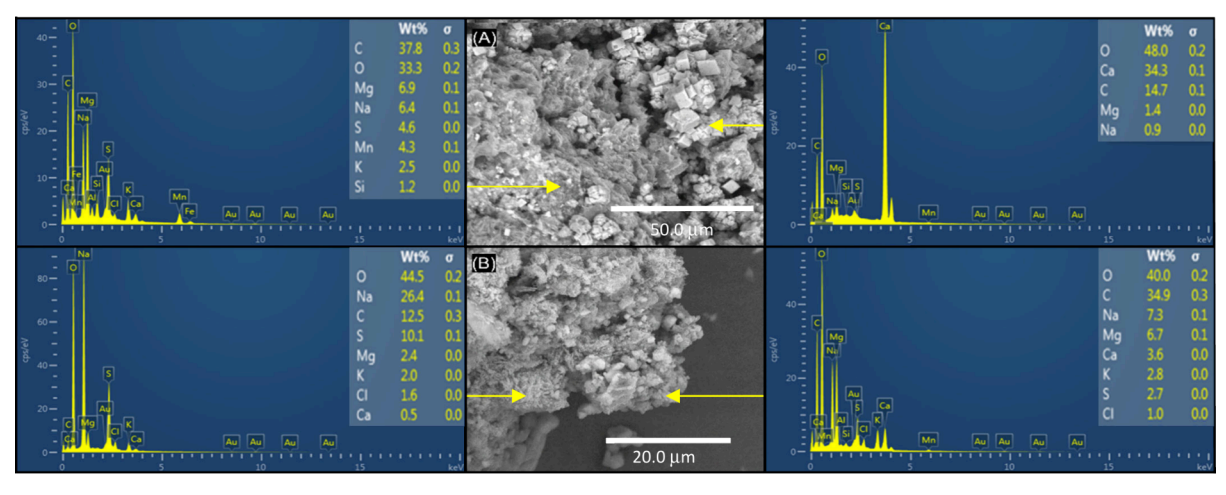


Figure 10. SEM images for the powders GLD in wastewater at 50 g/L (A) before and (B) after carbonation.

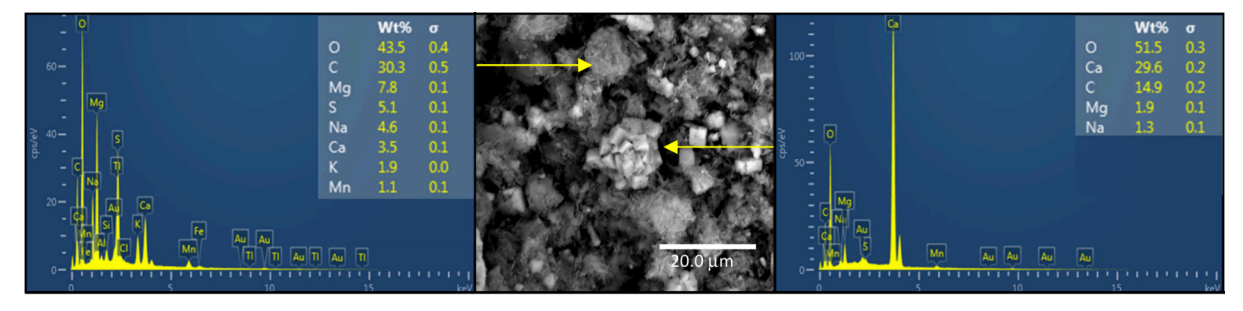


Figure 11. SEM images for the powders GLD in wastewater at 50 g/L after filtration and after carbonation.

Authors

Emmanouela Leventaki — Department of Chemistry and Chemical Engineering, Chalmers University of Technology, SE-41296 Gothenburg, Sweden Christian Kugge — R&D Centre, Svenska Cellulosa Aktiebolaget (SCA), SE-85121 Sundsvall, Sweden Diana Bernin — Department of Chemistry and Chemical Engineering, Chalmers University of Technology, SE-41296 Gothenburg, Sweden; © orcid.org/0000-0002-9611-2263 Complete contact information is available at: https://pubs.acs.org/10.1021/acssusresmgt.4c00373

Notes

The authors declare no competing financial interest.

ACKNOWLEDGMENTS

We acknowledge the Area of Advance Energy, Chalmers University of Technology and Energimyndigheten (P2021-00009) for financial support. The authors thank Svenska Cellulosa Aktiebolaget for the kind contribution in sourcing suitable material from industry. The authors also thank Carl Tryggers Stiftelse för Vetenskaplig Forskning for providing funding with the project "Instrumentation to utilize research on CO_2 capture to reach the climate goals".

REFERENCES

- (1) Bera, N.; Sardar, P.; Hazra, R.; Samanta, A. N.; Sarkar, N. Direct Air Capture of CO_2 by Amino Acid-Functionalized Ionic Liquid-Based Deep Eutectic Solvents. *ACS Sustain. Chem. Eng.* **2024**, *12*, 14288.
- (2) Bai, W. L.; Zhang, Y.; Wang, J. N. Continuous Capture and Reduction of CO₂ in an Electrochemical Molten-Salt System with High Efficiency. ACS Sustain. Chem. Eng. **2023**, 11 (42), 15364–15372.
- (3) Rubin, E. S.; Mantripragada, H.; Marks, A.; Versteeg, P.; Kitchin, J. The Outlook for Improved Carbon Capture Technology. *Prog. Energy Combust. Sci.* **2012**, *38* (5), 630–671.
- (4) Baena-Moreno, F. M.; Leventaki, E.; Riddell, A.; Wojtasz-Mucha, J.; Bernin, D. Effluents and Residues from Industrial Sites for Carbon Dioxide Capture: A Review. *Environ. Chem. Lett.* **2023**, *21* (1), 319–337.
- (5) Pan, S.; Shah, K. J.; Chen, Y.; Wang, M.; Chiang, P. Deployment of Accelerated Carbonation Using Alkaline Solid Wastes for Carbon Mineralization and Utilization Toward a Circular Economy. *ACS Sustain. Chem. Eng.* **2017**, *5*, 6429.
- (6) Huijgen, W.; Carbon Dioxide Sequestration by Mineral Carbonation, Energy Research Centre of the Netherlands, Wageningen University, The Netherlands, 2007 available at:http://edepot.wur.nl/121870.
- (7) Dubey, A.; Arora, A. Advancements in Carbon Capture Technologies: A Review. *J. Clean. Prod.* **2022**, 373, No. 133932.
- (8) Chen, Z.; Cang, Z.; Yang, F.; Zhang, J.; Zhang, L. Carbonation of Steelmaking Slag Presents an Opportunity for Carbon Neutral: A Review. *J. CO2 Util.* **2021**, *54* (July), No. 101738.
- (9) Chen, T.; Chen, Y.; Dai, M.; Chiang, P. Stabilization-Solid-ification-Utilization of MSWI Fly Ash Coupling CO₂ Mineralization Using a High-Gravity Rotating Packed Bed. *Waste Manag* **2021**, *121*, 412–421.
- (10) Huang, X.; Zhang, J.; Zhang, L. Accelerated Carbonation of Steel Slag: A Review of Methods, Mechanisms and Influencing Factors. *Constr. Build. Mater.* **2024**, *411*, No. 134603.
- (11) Baciocchi, R.; Costa, G.; Di Bartolomeo, E.; Polettini, A.; Pomi, R. The Effects of Accelerated Carbonation on CO₂ Uptake and Metal Release from Incineration APC Residues. *Waste Management* **2009**, 29 (12), 2994–3003.
- (12) Baena-moreno, F. M.; Cid-castillo, N.; Arellano-garcía, H.; Reina, T. R. Science of the Total Environment Towards Emission Free Steel Manufacturing Exploring the Advantages of a CO₂ Methanation Unit to Minimize CO₂ Emissions. *Sci. Total Environ* **2021**, 781, No. 146776.
- (13) Luo, W.; Li, B.; Xu, M.; Pang, C.; Lester, E.; Xu, L.; Kow, K. Science of the Total Environment In-Situ Release and Sequestration of CO_2 in Cement Composites Using LTA Zeolites. *Sci. Total Environ.* **2023**, 872, 162133.
- (14) Kinnarinen, T.; Golmaei, M.; Jernström, E.; Häkkinen, A. Separation, Treatment and Utilization of Inorganic Residues of Chemical Pulp Mills. *J. Clean. Prod.* **2016**, *133*, 953–964.
- (15) Eugenio, M. E.; Ibarra, D.; Martín-Sampedro, R.; Espinosa, E.; Bascón, I.; Rodríguez, A.Alternative raw materials for pulp and paper

- production in the concept of a lignocellulosic biorefinery, *Cellulose*. Springer: Berlin, Germany,2019.
- (16) dos Santos, V. R.; Cabrelon, M.D.; de Sousa Trichês, E.; Quinteiro, E. Green Liquor Dregs and Slaker Grits Residues Characterization of a Pulp and Paper Mill for Future Application on Ceramic Products. J. Clean. Prod. 2019, 240,118220. DOI: 10.1016/j.jclepro.2019.118220
- (17) Mäkitalo, M. Green Liquor Dregs as Sealing Layer Material to Cover Sulphidic Mine Waste Deposits. Thesis, Luleå University of Technology, Luleå, Sweden, 2012.
- (18) Mäkitalo, M.; Maurice, C.; Jia, Y.; Öhlander, B. Characterization of Green Liquor Dregs, Potentially Useful for Prevention of the Formation of Acid Rock Drainage 2014, 4, 330–344.
- (19) Spínola, A. C.; Pinheiro, C. T.; Ferreira, A. G. M.; Gando-Ferreira, L. M. Mineral Carbonation of a Pulp and Paper Industry Waste for CO₂ Sequestration. *Process Saf. Environ. Prot.* **2021**, 148, 968–979.
- (20) Han, S. J.; Yoo, M.; Kim, D. W.; Wee, J. H. Carbon Dioxide Capture Using Calcium Hydroxide Aqueous Solution as the Absorbent. *Energy Fuels* **2011**, 25 (8), 3825–3834.
- (21) Yoo, M.; Han, S. J.; Wee, J. H. Carbon Dioxide Capture Capacity of Sodium Hydroxide Aqueous Solution. *J. Environ. Manage.* **2013**, *114*, 512–519.
- (22) Leventaki, E.; Baena-Moreno, F. M.; Sardina, G.; Strom, H.; Ghahramani, E.; Naserifar, S.; Ho, P. H.; Kozlowski, A. M.; Bernin, D. In-Line Monitoring of Carbon Dioxide Capture with Sodium Hydroxide in a Customized 3D-Printed Reactor without Forced Mixing. Sustainability 2022, 14, 10795.
- (23) Giacomin, C. E. Fluidized Calcium Carbonate Crystallization in Alkaline Liquids. 2019, pp 1-99.
- (24) Ragipani, R.; Sreenivasan, K.; Anex, R. P.; Zhai, H.; Wang, B. Direct Air Capture and Sequestration of CO₂ by Accelerated Indirect Aqueous Mineral Carbonation under Ambient Conditions. *ACS Sustain. Chem. Eng.* **2022**, *10*, 7852.
- (25) Zhai, H.; Chen, Q.; Yilmaz, M.; Wang, B. Enhancing Aqueous Carbonation of Calcium Silicate through Acid and Base Pretreatments with Implications for Efficient Carbon Mineralization. *Environ. Sci. Technol.* **2023**, *57*, 13808.
- (26) Jia, Y.; Hamberg, R.; Qureshi, A.; Mäkitalo, M.; Maurice, C. Variation of Green Liquor Dregs from Different Pulp and Paper Mills for Use in Mine Waste Remediation. *Environ. Sci. Pollut. Res.* **2019**, 26 (30), 31284–31300.
- (27) de Oliveira, A. I.; Subhani, M.; Aramburu, A. B.; Rossetto, H. L.; Trindade, G. H.; dos Santos, W. J.; de Avila Delucis, R. Use of Dregs as a Replacement for Hydrated Lime in Cement Coating Mortar. *J. Compos. Sci.* **2023**, *7* (5), 181.
- (28) Srivastava, S.; Moukannaa, S.; Isteri, V.; Ramteke, D. D.; Perumal, P.; Adesanya, D.; Kinnunen, P.; Ohenoja, K.; Illikainen, M. Utilization of Calcite-Rich Green Liquor Dregs (GLD) by-Products from Pulp and Paper Industry: Cement Clinker Production and Life Cycle Analysis. *Case Stud. Constr. Mater.* **2024**, 20, No. e02870.
- (29) Gerard, A.; Muhr, H.; Plasari, E.; Jacob, D.; Lefaucheur, C. E. Effect of Calcium Based Additives on the Sodium Bicarbonate Crystallization in a MSMPR Reactor. *Powder Technol.* **2014**, 255, 134–140.
- (30) Cheng, W.; Fang, L.; Cheng, H.; Li, E.; Zhang, C.; Cheng, F. Formation of $MgCO_3\cdot 3H_2O$ in the CO_2 Mineralization System Using $Mg(OH)_2$ as an Intermediate at 20° C. *J. Ind. Eng. Chem.* **2019**, 76, 215–222.